10168–10177 *Nucleic Acids Research, 2017, Vol. 45, No. 17* *Published online 2 August 2017*
doi: 10.1093/nar/gkx694

The kinetic mechanism of bacterial ribosome recycling

Yuanwei Chen[1], Akira Kaji[2,*], Hideko Kaji[3] and Barry S. Cooperman[1,*]

[1]Department of Chemistry, University of Pennsylvania, Philadelphia, PA 19104, USA, [2]Department of Microbiology, Perelman School of Medicine, University of Pennsylvania, Philadelphia, PA 19104, USA and [3]Department of Biochemistry and Molecular Biology, Jefferson Medical College, Thomas Jefferson University, Philadelphia, PA 19137, USA

Received April 28, 2017; Revised July 24, 2017; Editorial Decision July 25, 2017; Accepted July 26, 2017

ABSTRACT

Bacterial ribosome recycling requires breakdown of the post-termination complex (PoTC), comprising a messenger RNA (mRNA) and an uncharged transfer RNA (tRNA) cognate to the terminal mRNA codon bound to the 70S ribosome. The translation factors, elongation factor G and ribosome recycling factor, are known to be required for recycling, but there is controversy concerning whether these factors act primarily to effect the release of mRNA and tRNA from the ribosome, with the splitting of the ribosome into subunits being somewhat dispensable, or whether their main function is to catalyze the splitting reaction, which necessarily precedes mRNA and tRNA release. Here, we utilize three assays directly measuring the rates of mRNA and tRNA release and of ribosome splitting in several model PoTCs. Our results largely reconcile these previously held views. We demonstrate that, in the absence of an upstream Shine–Dalgarno (SD) sequence, PoTC breakdown proceeds in the order: mRNA release followed by tRNA release and then by 70S splitting. By contrast, in the presence of an SD sequence all three processes proceed with identical apparent rates, with the splitting step likely being rate-determining. Our results are consistent with ribosome profiling results demonstrating the influence of upstream SD-like sequences on ribosome occupancy at or just before the mRNA stop codon.

INTRODUCTION

Ribosomes catalyze protein synthesis, a vital cellular activity that can be divided into four major steps: initiation, elongation, termination and ribosome recycling. During termination, the completed polypeptide chain bound to a transfer RNA (tRNA) in the P-site of the ribosome within the pre-termination complex (PreTC) is released from the tRNA by the hydrolytic action of a release factor bound to a stop codon in the adjacent A-site. The resulting post-termination complex (PoTC) contains the now deacylated tRNA still bound in the P-site and the messenger RNA (mRNA) that encoded the polypeptide chain. Recycling of prokaryotic PoTC is catalyzed by the concerted actions of two essential proteins (1,2), ribosome recycling factor (RRF) and the guanosine triphosphate (GTP) complex of elongation factor G (EF-G), the latter being a factor that is also critical for polypeptide elongation.

Although the recycling requirement for both RRF and EF-G·GTP has been known for some time (3), the detailed mechanism by which the two factors effect PoTC breakdown remains controversial (4). One view holds that the principal biological role of RRF and EF-G·GTP in catalyzing recycling is to effect the release of mRNA and tRNA from the PoTC (5,6) with the splitting of the 70S ribosome into 30S and 50S subunits being somewhat dispensable. This view has been strengthened by three recent publications showing first, that *Escherichia coli* containing ribosomes whose subunits are linked covalently, rendering them unsplittable and are able to grow with 60% efficiency compared to wild-type (7); second, that $\geq$50% of protein synthesis initiation events occur on 70S ribosomes rather than on 30S subunits (8) and third, that neither *in vitro* nor *in vivo* expression of the second cistron of a bicistronic mRNA requires the presence of active RRF (9). According to the second view, which is based on rate measurement studies on model PoTCs (10–14), it is catalysis of the splitting reaction, which precedes mRNA and tRNA release, which is the principal role of RRF and EF-G·GTP.

Complicating attempts to resolve this controversy have been the differences in both the PoTC model systems used for *in vitro* studies by the various groups and the measurements utilized in reaching conclusions about the recycling

*To whom correspondence should be addressed. Tel: +215 898 6330; Email: cooprman@pobox.upenn.edu
Correspondence may also be addressed to Akira Kaji. Tel: +215 370 9799; Email: kaji@mail.med.upenn.edu
Present address: Yuanwei Chen, 1600 Amphitheatre Parkway, Mountain View, CA 94043, USA.

mechanism. In addition, there has been a lack of clarity concerning the full consequences for the kinetic mechanism of recycling of including a purine-rich six-base sequence, known as a Shine–Dalgarno (SD) sequence, proximally upstream of the deacylated tRNA codon (11–13). The SD sequence increases mRNA affinity for the ribosome via base-pairing with a pyrimidine-rich sequence at the 3′-end of 16S rRNA (15). The potential importance of SD-like sequences for recycling is suggested by the results of ribosome profiling studies demonstrating the prevalence of such sequences near the stop codons of transcription attenuation leader peptides (16) and within operons that are closely followed by a downstream gene (17). Such proximity increases the likelihood that SD-like sequences, by modulating ribosome recycling, can both prevent the formation of anti-termination stem-loops, thereby ensuring proper transcription termination (16) and enhance the re-initiation of translation at distal genes in operons (17).

Here we utilize three assays that directly measure the rates of mRNA and tRNA release and ribosome splitting in model PoTCs formed using mRNAs that either lack or contain a proximal upstream SD sequence, denoted the 'common case' and the 'SD-case', respectively. We demonstrate that, in the common case, PoTC breakdown proceeds in the order: mRNA release followed by tRNA release and then by 70S splitting, whereas in the SD-case all three processes proceed with identical apparent rates. We also discuss the biological significance of these kinetic schemes and possible reasons for the differences between our conclusions and those put forward by others earlier.

MATERIALS AND METHODS

More detail is provided in Supplementary Data.

Materials

Materials were either obtained commercially or prepared by standard methods. mRNAs are listed in Table 1. Both $tRNA^{Phe}$ and $tRNA^{Gly}$ were prepared from yeast.

Complex preparation

PreTC was prepared by incubating ribosomes (1 μM) with mRNA (2 μM) and N-AcPhe-$tRNA^{Phe}$ (2 μM) in Buffer P [50 mM Tris–HCl (pH 7.6), 80 mM NH_4Cl, 10 mM $MgSO_4$ and 0.2 mM dithiothreitol (DTT)] for 1 h at 37°C. After incubation, unbound RNAs were removed by centrifugation at 15 000 rpm and 4°C with an Amicon-Microcon spin column (Millipore, with 30 kD cutoff). The remaining solution was diluted in Buffer A (50 mM Tris–HCl (pH 7.6), 80 mM NH_4Cl, 5 mM $MgSO_4$ and 0.2 mM DTT) and stored frozen in aliquots.

PoTC was prepared similarly, except that deacylated $tRNA^{Phe}$ or $tRNA^{Gly}$ was used in place of AcPhe-$tRNA^{Phe}$ and Buffer A replaced Buffer P. PoTC was either used immediately after preparation in stopped-flow experiments or kept on ice for steady-state measurements made within 2 h after preparation.

To determine the stoichiometry of $tRNA^{Phe}$ bound per ribosome, PoTC was prepared by incubating ribosomes (1 μM) in Buffer A for 1 h at 37°C with [^{32}P]-$tRNA^{Phe}$ (2 μM) in the presence of either the cognate mRNA-F7 (2 μM) or mRNA-fMet-STOP (2 μM), which lacks a UUC or UUU triplet cognate to $tRNA^{Phe}$ (see sequence in Supplementary Data). After incubation, unbound tRNAs were removed by centrifugation at 15 000 rpm and 4°C for 30 s using an Amicon-Microcon spin column (Millipore, 30 kD cutoff). The amount of tRNA and ribosomes in the supernatant was determined by scintillation counting and A_{260} measurement (1 A_{260} unit = 26 pmol ribosome), respectively.

Fluorescence and light scattering measurements

Both steady-state and stopped-flow fluorescence anisotropy and light scattering measurements were carried out in Buffer A at 37°C.

Steady-state fluorescence anisotropy. Experiments were conducted on a Fluorolog-3 spectrofluorometer (Horiba Jobin Yvon). Both proflavin- and fluoroscein-labeled samples were excited at 462 nm, with fluorescence emission monitored at 512 and 492 nm, respectively. Fluorescence anisotropy was measured using an L-format as described (18).

Stopped-flow experiments. Rate experiments were performed on a KinTek SF-300X stopped-flow spectrofluorometer. The indicated concentrations of all components are final after mixing. GTP was present at 0.5 mM when utilized. Apparent rate constants (k_{app}) were determined by fitting results to Equation (1) for each independent experiment, using Origin (OriginLab).

$$A(t) = A_0 + A_1 \times e^{-kt} \quad (1)$$

Fluorescence anisotropy. Both proflavin- and fluoroscein-labeled samples were excited at 462 nm and fluorescence was monitored using a pair of 495 nm long-pass filters. thG was excited at 340 nm and monitored using a pair of 425 nm long-pass filters. Fluorescence anisotropy was measured using a T-format as described (18,19).

Light scattering was measured as described (20). Excitation was at 436 nm and output was monitored without using a filter.

RESULTS

mRNA and tRNA binding to the ribosome can be monitored by increases in fluorescence anisotropy

The fluorescence anisotropies of fl-mRNA-F7 and fl-mRNA-F10 (Table 1) increase on binding to a 70S ribosome, but the increase for fl-mRNA-F7 at saturating ribosome concentration (Supplementary Figure S1A) is about double that for fl-mRNA-F10 (data not shown), likely because the fluorescein fluorophore within the mRNA channel is more tightly bound at position +7 than at position +10. This larger change led us to choose fl-mRNA-F7 for many of the studies reported below. The results displayed in Supplementary Figure S1A allowed calculation of K_d values of 0.016 and 0.075 μM for fl-mRNA-F7 binding to 70S ribosomes in the presence and absence of cognate

Table 1. mRNA sequences[a]

mRNA	Sequence
mRNA-F7	AUAGCAUCACAUAUC**UUCUAA**C
fl-mRNA-F7	AUAGCAUCACAUAUC**UUCUAA**C-fl[d]
fl-mRNA-F10	AUAGCAUCACAUAUC**UUCUAA**CAGU-fl
mRNA-thG[b]	AUACGAUCACAUA**thGCUUCUAA**CAUGCCGGCCAUCCAAAC
mRNA-G7	AUAGCAUCACAUAUC**GGCUAA**C
fl-mRNA-G7	AUAGCAUCACAUAUC**GGCUAA**C-fl
mRNA-SD-F7[c]	AUA**AGGAGG**UAAAA**UUCUAA**C
fl-mRNA-SD-F7[c]	AUA**AGGAGG**UAAAA**UUCUAA**C-fl
mRNA-fMet-Stop	GGGAAUCCAAAAAUCUAAAAGUUAACUACAUACUA**UGUAA**CGAUUACUAGAU CUCCUCCACUUAACGCGUCUGCAGGCAUGCAAGCU(A)$_{26}$GCUUG

[a]Cognate sequences to deacylated tRNAs and adjacent UAA stop codons are in bold.
[b] thG position is in bold.
[c]Upstream SD sequence is in bold.
[d]fl, fluorescein

tRNA^{Phe}, respectively. Similar results were obtained for other fluorescent-labeled mRNAs employed in this study (mRNA-thG, fl-mRNA- G7, fl-mRNA-SD-F7, Supplementary Table S1). The SD sequence AGGAGG, located 9–14 nt upstream of the stop codon (mRNA-SD-F7, Table 1), increases the strength of mRNA binding to the ribosome, as measured by fluorescence anisotropy, and the magnitude of the anisotropy change that accompanies binding (Supplementary Table S1).

Fluorescence anisotropy can also be used to measure proflavin-labeled tRNA^{Phe} [tRNA^{Phe}(prf)] binding to the ribosome (21). Since deacylated tRNA has a much higher affinity for the P-site than for either the A-site or the E-site (22–24), and, compared with *E. coli* tRNA^{Phe}, the yeast tRNA^{Phe} utilized in this work has an equivalent P-site affinity but a much lower E-site affinity (23,24), such binding is expected to be primarily to the P-site. In accord with this expectation, the tRNA^{Phe}(prf) binding we measure by fluorescence anisotropy is strongly codon-dependent, as shown by the 4-fold lower anisotropy change observed when mRNA-F7 is replaced by non-cognate mRNA-G7 (Supplementary Figure S1B). These anisotropy results are fully consistent with results measuring the stoichiometry of [^{32}P]-tRNA^{Phe} bound to a PoTC prepared with cognate mRNA-F7 (0.85/ribosome) versus the value of 0.23/ribosome found when non-cognate mRNA-fMet-STOP replaced mRNA-F7. Such codon dependence is characteristic of P-site binding. In contrast, E-site binding is essentially codon independent (22–25).

RRF/EF-G-induced breakdown of common post-termination complexes (PoTCs)

In earlier studies of ribosome recycling kinetics, PoTC complexes prepared either by release of peptide from pre-termination complexes or by direct binding of deacylated tRNA showed no differences in the results obtained (12,13). In this work, we used the latter method to prepare three nearly identical PoTCs containing 70S ribosomes and mRNAs lacking an upstream SD sequence, which we define as common PoTCs. These PoTCs, containing either fl-mRNA-F7 and tRNA^{Phe} (denoted PoTC-F7-fl), or mRNA-F7 and tRNA^{Phe}(prf) (denoted PoTC-F7-prf), or mRNA-F7 and tRNA^{Phe} (denoted PoTC-F7), were used to determine rates of the three processes, mRNA release, tRNA release and 70S splitting, which occur during RRF and EF-G·GTP-dependent PoTC breakdown. Decreases in the fluorescence anisotropies of PoTC-F7-fl (Figure 1A and D) and PoTC-F7-prf (Figure 1B and E) were used to measure monophasic rates of mRNA release (k_{mRNA}, Supplementary Figure S2A and D) and tRNA release (k_{tRNA}, Supplementary Figure S2B and E), respectively. Decreases in light scattering (12) measured monophasic rates of 70S splitting (k_{split}, Figure 1C and F; Supplementary Figure S2C and F). The results displayed in Figure 1C and F were obtained using PoTC-F7, but essentially identical results were obtained using PoTC-F7-fl or PoTC-F7-prf. For all three measurements, no such decreases were seen if a PreTC, containing N-AcPhe-tRNA^{Phe} in place of tRNA^{Phe}, was mixed with RRF and EF-G·GTP, consistent with the known failure of RRF to bind to a ribosome containing P-site bound peptidyl-tRNA (26–29).

Suitable control experiments showed that mRNA and tRNA release proceeded much more slowly (two to three orders of magnitude) and to lesser extents in the presence of either RRF or EF-G·GTP alone, or in the absence of both factors (Supplementary Figure S3A and B). Rapid mixing of PoTC-F7-fl with a large molar excess of unlabeled mRNA-F7 also led to fl-mRNA-F7 release (Supplementary Figure S3C), demonstrating that mRNA bound within the PoTC is in mobile equilibrium with mRNA in solution, in agreement with earlier results of Peske *et al.* (13), but the rate of release is some 10-fold lower than what was found by mixing with RRF (2 μM) and EF-G·GTP (3 μM) (Figure 1A and D). Above we have summarized the evidence that deacylated tRNA binding in our model PoTC complex occurs primarily to the P-site rather than to the E-site. The result that all of the traces of deacylated tRNA release as a function of time (Figure 1B and E; Supplementary Figure S2B and E) are well fit by single exponentials provides additional evidence that E-site binding is minimal, since satisfactory fitting of tRNA release traces would likely require two exponentials if E-sites were occupied to a significant extent.

The results presented in Figure 1 permitted determination of two sets of k_{app} values for each process, one at fixed EF-G (3.0 μM) and varying RRF concentrations (Figure 1A–C) and the other at fixed RRF (2.0 μM) and varying

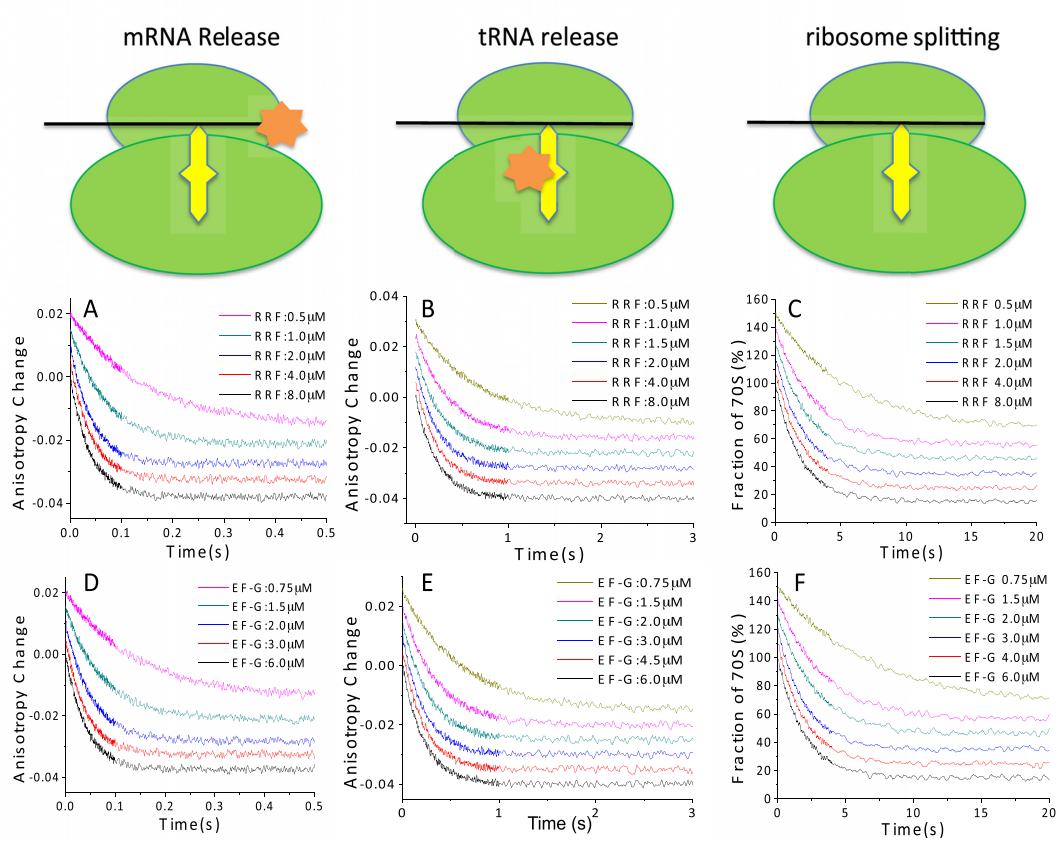

Figure 1. Rates of RRF/EF-G-induced PoTC-F7 breakdown. As measured by the decrease in the fluorescein (star) anisotropy of fl-mRNA-F7 (**A** and **D**) or the proflavin (star) anisotropy of $tRNA^{Phe}$(prf) (**B** and **E**) or light scattering (**C** and **F**) on rapid mixing of PoTC-F7 (0.2 μM) with EF-G·GTP and RRF. (A–C) EF-G·GTP (2 μM) and varying concentrations of RRF. (D–F) RRF (3 μM) and varying concentrations of EF-G·GTP. 70S is fully associated (100%) at zero time for all curves in (C) and (F), as indicated at the highest concentrations of RRF (8 μM) and EF-G (6 μM), respectively. For clarity, the 100% values at zero time are offset by 10% for each lowering of RRF and EF-G concentrations. In both (C) and (F), association decreased to 15% at 20 s for all but the lowest concentrations of RRF (0.5 μM) and EF-G (0.75 μM).

EF-G concentrations (Figure 1D–F). These values were fit to the Michaelis–Menten equation (Equation 2), where F is either EF-G or RRF. The K_m values for each protein factor measured for each of the three processes were essentially identical, although somewhat lower for RRF than for EF-G (K_m^{RRF} 0.7–0.8 μM; $K_m^{EF\text{-}G}$ 1.1–1.2 μM). The two k_{cat} values determined for each process in both sets were identical, but the three processes within each set had k_{cat} values that differed markedly from one another (Supplementary Table S2). These latter values ($k_{cat,mRNA}$ 26 ± 3 s^{-1}; $k_{cat,tRNA}$ 4.7 ± 0.3 s^{-1}; $k_{cat,split}$ 0.58 ± 0.04 s^{-1}) demonstrate clearly that breakdown of the PoTC proceeds in the following order: mRNA release, tRNA release and ribosome splitting.

$$k_{app} = k_{cat}[F]/(K_m^F + [F]) \quad (2)$$

The generality of this conclusion for model PoTC breakdown could be limited by two possible concerns. The first is that in fl-mRNA-F7, the sequence corresponding to the 3′-untranslated region of mRNA (3′-UTR) following the stop codon is only 1 nt long. This is a consequence of placing the fluorescent label at the 3′-end at the +7 position from the P-site so that it yields an easily measurable anisotropy change on binding to the ribosome, presumably because at position +7 the label is held tightly within the mRNA channel. Could mRNA dissociation be unusually fast because of the shortness of the 3′-UTR? Second, could the slightly different PoTCs used in obtaining the results in Figure 1, necessary because of the overlap in the emission spectra of fluorescein and proflavin, affect the kinetic order of the three events?

To confront these concerns, we carried out an additional set of PoTC breakdown experiments using an additional common PoTC, denoted PoTC-thG-prf. PoTC-thG-prf contains an mRNA, denoted thG-mRNA, in which the emissive, isosteric guanosine surrogate thG (30,31) is placed at the −2 position from the P site. It also has an 18-nt long 3′-UTR, more than enough to completely fill the mRNA channel. In addition, because thG emission is easily distinguishable from proflavin emission, and light scattering change could be monitored at a wavelength different from both emissions, all three processes could be monitored using the same PoTC sample. The results, measured at near saturating concentrations of RRF and EF-G (Figure 2A), are virtually identical to those obtained using mRNA-F7 or fl-mRNA-F7 (Table 2). We conclude that neither of the potential concerns mentioned above is problematic for model PoTC breakdown and that generally valid kinetic results are obtained with the shorter mRNAs, mRNA-F7 and its flu-

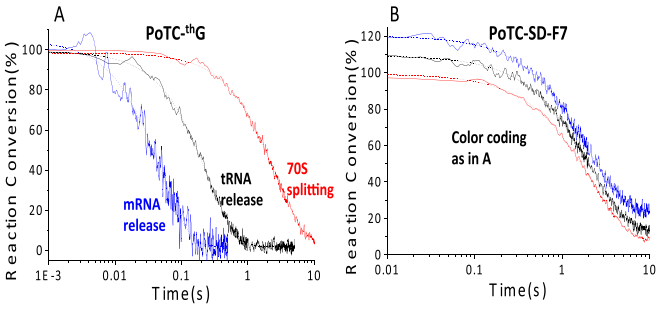

Figure 2. Direct comparisons of rates of RRF/EF-G-induced PoTC (0.2 μM) breakdown on rapid mixing with 3 μM EF-G·GTP and 2 μM RRF. (**A**) PoTC-thG, as measured by the decrease in mRNA-thG anisotropy (blue line), tRNA^{Phe}(prf) anisotropy (black line) or light scattering (red line). (**B**) PoTC-SD-F7, tRNA^{Phe}(prf) anisotropy (black line) or light scattering (red line); PoTC-SD-F7-fl, mRNA-thG anisotropy (blue line). Initial values of mRNA and tRNA anisotropy are offset by +20 and +10%, respectively, for clarity.

orescent derivative, fl-mRNA-F7. Consequently, these mRNAs are employed in the studies described below except as otherwise noted.

Modulation of RRF/EF-G-induced common PoTC breakdown

Having established the kinetic mechanism of breakdown for common PoTCs, we turned our attention to determining how changes in a variety of pertinent reaction variables, or in the identity of the tRNA contained in the PoTC, affect values of k_{mRNA}, k_{tRNA} and k_{split}, as presented in Table 2.

Added initiation factor 3 (IF3). IF3 binds 30S subunits more tightly than 70S ribosomes (32) and there is general agreement in the literature that IF3 aids RRF/EF-G stimulation of ribosome splitting during PoTC breakdown only indirectly, by preventing the reassociation of subunits after ribosome splitting (11,12,33), rather than by a direct interaction with the 70S ribosome, as proposed originally (10,13). However, there has been disagreement over whether IF3 stimulates mRNA and tRNA dissociation during ribosome recycling. Our rate measurements (Table 2) clearly show that while IF3 has no effect on the rate of either mRNA or tRNA dissociation, it does have a minor effect in slightly increasing the extent of ribosome splitting, from 85 ± 4 to 98 ± 3% (Supplementary Figure S4A). In addition, close inspection of the time dependence of ribosome splitting shows that it is better fit as a biphasic exponential change, in which the major, more rapid phase has a k_{split} value indistinguishable from that measured in the absence of IF3 (Table 2). We attribute the minor slower phase to the effect of IF3 in inducing further ribosome splitting via its preferential binding to the 30S subunit.

Is GTP hydrolysis necessary? Although EF-G is clearly necessary for PoTC breakdown, prior to the present work there were no data available unambiguously indicating whether GTP hydrolysis is required for either mRNA or tRNA release. To address this question we carried out our standard three rate measurements, but substituting either guanosine diphosphate (GDP) or GDPNP, a non-hydrolyzable GTP analog in which the oxygen bridging the beta and gamma phosphoryl groups is replaced by an NH, for GTP. None of the reactions proceed when GDP replaces GTP, and no splitting is observed when GDPNP replaces GTP. This latter result confirms earlier observations that GTP hydrolysis is required for ribosome splitting (11,13,14,34). In contrast, neither the rate (Table 2) nor the extent of tRNA dissociation is affected by substituting GDPNP for GTP. Such substitution has an intermediate effect on mRNA, reducing both the extent and rate of mRNA-F7 release from the PoTC (Supplementary Figure S4B), and, in complementary fashion, permitting partial binding of mRNA-F7 to 70S ribosomes, a process that is almost completely prevented in the presence of GTP (Supplementary Figure S5). These results indicate that both tRNA and mRNA release from the PoTC requires binding of EF-G in the EF-G·GTP conformation (35,36) and that, while mRNA release is significantly hindered in the absence of GTP hydrolysis, tRNA release is unaffected.

Antibiotic inhibition. The antibiotics fusidic acid (FA), thiostrepton (ThS) and viomycin (Vio) are known to inhibit mRNA and tRNA release (37) and ribosome splitting (14) during PoTC breakdown. Hirokawa *et al.* (37) have argued that comparing K_i values for the three steps permits an inference as to the order in which the steps occur, with the slowest step having the lowest K_i and the fastest step having the highest K_i. This conclusion is based on the assumption that a given antibiotic captures a competent intermediate in PoTC breakdown. Since ribosome splitting is the slowest step in our standard assay, the vacant 70S ribosome is a competent intermediate, and a concentration of an antibiotic sufficient to inhibit splitting would be insufficient to inhibit either mRNA or tRNA dissociation. Accordingly, these steps would necessarily have higher K_i values. We determined apparent K_i values under our standard assay conditions, giving the results summarized in Table 3. These values clearly support our results showing that mRNA and tRNA dissociation precede ribosome splitting, but don't allow a clear inference regarding the order of mRNA versus tRNA dissociation. The values of K_i determined by Hirokawa *et al.* (37) for mRNA and tRNA release are also shown in Table 3. We defer consideration of differences in the two sets of results to the 'Discussion' section.

tRNA identity. PoTCs formed *in vivo* will, in the aggregate, contain a distribution of all elongator tRNA isoacceptors, raising the question of whether the identity of the elongator tRNA, tRNA^{Phe} in the above studies, might influence the order of PoTC breakdown, due perhaps to differences in the thermodynamic stabilities of codon:anticodon base pairing. We examined this question by comparing PoTC breakdown rates when the UUC codon in mRNA-F7, which forms one G–C base pair with its cognate tRNA^{Phe}, is replaced by a GGC codon in mRNA-G7, which forms three G–C base pairs with its cognate tRNA$^{Gly}_{GCC}$ isoacceptor. This substitution does not change the order of PoTC breakdown but reduces the rates of both mRNA release and tRNA release by 1.5- to 1.8-fold (Table 2). While the reduced rate of

Table 2. Apparent rate constants (s^{-1})[a]

mRNA/tRNA	Variable	k_{mRNA}[c]	k_{tRNA}	k_{split}
F7/Phe		25 ± 1	4.3 ± 0.2	0.47 ± 0.04[e]
thG/Phe		26 ± 2	4.1 ± 0.3	0.39 ± 0.05
G7/Gly		13.8 ± 0.8	2.9 ± 0.2	0.44 ± 0.02
SD-F7/Phe		0.51 ± 0.04	0.53 ± 0.04	0.50 ± 0.04
F7/Phe	2 μM IF3	25 ± 1	4.4 ± 0.3	0.50 ± 0.03[f] 0.12 ± 0.02
	0.5 mM GDPNP[b]	11 ± 1[d]	4.3 ± 0.2	No reaction
	7.5 mM Mg^{2+}	3.6 ± 0.1	0.49 ± 0.03	0.074 ± 0.004
	3 mM Mg^{2+}	n.d.	n.d.	2.8 ± 0.1
	Non-His tagged EF-G	25 ± 1	4.2 ± 0.3	0.30 ± 0.03

[a]Standard conditions: 2 μM RRF, 3 μM His-tagged EF-G, 5 mM Mg^{2+}, 0.5 mM GTP. Error ranges are standard deviations for 3–10 independent measurements.
[b]Replaces GTP.
[c]mRNA dissociation rates were measured with fl-F7-mRNA, fl-G7-mRNA, fl-SD-F7-mRNA or thG-mRNA.
[d]Partial release of mRNA.
[e]There was no significant difference in measured rate constant when fl-mRNA-F7 replaced mRNA-F7 or when Phe-tRNA^{Phe}(prf) replaced Phe-tRNA^{Phe}.
[f]Major reaction phase (amplitude 77 ± 6% of total change).

Table 3. Apparent K_i values (μM)[a]

Antibiotic	mRNA dissociation	tRNA dissociation	70S splitting
Thiostepton	23 ± 2	16 ± 2	3.3 ± 0.8
	12.5[c]	92.3[c]	6[d]
Viomycin	2.0 ± 0.4	1.8 ± 0.2	0.6 ± 0.1
	25[c]	58.3[c]	50[d]
Fusidic acid	No inhibition[b]	No inhibition[b]	<0.5
	10[c]	No inhibition[c]	15[d]

[a]Values are for this work, standard conditions as in Table 2, unless otherwise indicated.
[b]Measured at 100 μM FA.
[c]ref. (37);
[d]ref. (33).

mRNA release might well be a consequence of more stable codon:anticodon base pairing, the reduced rate of tRNA release, which follows mRNA release, must reflect differential interactions with the ribosome of tRNA$^{Gly}_{GCC}$ versus tRNA^{Phe}. As expected, the rate of ribosome splitting is the same for the two complexes, since splitting only occurs following mRNA and tRNA dissociation. This suggests that the kinetic order of the rate processes in PoTC breakdown is likely to be the same for all elongator tRNAs.

Other variables. Some other studies of PoTC breakdown have employed higher Mg^{2+} concentrations than the 5 mM we employ in our standard assay. Accordingly, for comparison purposes, we determined the effects of raising Mg^{2+} concentration on PoTC breakdown. The results demonstrate that the rates of all three processes were much reduced (5- to 7-fold) at the higher (7.5 mM) Mg^{2+} concentration. Conversely, lowering Mg^{2+} to 3.0 mM raised the rate of ribosome splitting 6-fold (Table 2). This very marked increase in the rate of 70S splitting as [Mg^{2+}] is lowered from 7.5 to 3.0 mM is similar to what has been observed previously for uncatalyzed splitting of vacant 70S ribosomes (38). Lastly, we showed that replacing the N-terminal His-tagged EF-G we use in our standard assay with native EF-G directly prepared from *E. coli* cells has only a small effect on k_{split} and no effect on either k_{mRNA} or k_{tRNA} (Table 2).

RRF/EF-G-induced breakdown of a PoTC containing an upstream SD sequence

Some prior studies of recycling have employed model PoTCs made with mRNAs containing upstream SD sequences (12,13), raising the question of whether such sequences might influence the mechanism of ribosome recycling (4). Although an upstream SD sequence does not affect the rate of ribosome splitting (12), no results have been reported directly measuring the relative effects of an upstream SD sequence on the kinetics of mRNA or tRNA release from a PoTC. To fill this gap, we compared PoTC breakdown rates for complexes made with an mRNA containing an upstream SD sequence (mRNA-SD-F7 or fl-mRNA-SD-F7) with those determined above for mRNA-F7 and fl-mRNA-F7 (Table 2).

The inclusion of the upstream SD sequence in fl-mRNA-SD-F7 results in a 7-fold higher affinity for the ribosome versus fl-mRNA-F7 (Supplementary Table S1) and decreased rates of both mRNA (50-fold) and tRNA release (10-fold), consistent with an earlier study showing that SD–anti-SD interactions strengthen binding of mRNA and tRNA to the PoTC (11). In contrast, the rate of ribosome splitting is unchanged by the presence of the upstream SD sequence, also in agreement with prior results (12,13). Importantly, the rates of all three processes measured with either mRNA-SD-F7 or fl-mRNA-SD-F7 are equal to each other (Figure 2B), suggesting that all three processes have a

common rate-determining step. A plausible interpretation of these results is that the presence of the upstream SD sequence significantly alters the kinetic sequence of PoTC breakdown, such that rate-determining ribosome splitting is followed by rapid release of mRNA and tRNA from the 30S subunit (see 'Discussion' section).

DISCUSSION

PoTC breakdown requires the combination of RRF and EF-G to catalyze three dissociation processes, mRNA and tRNA release and splitting of the 70S ribosome into 30S and 50S subunits. In this paper, we present the first study that reports parallel rate measurements of all three processes for common model PoTCs that lack a SD sequence immediately upstream of the termination codon and that, moreover, directly measure mRNA release. Our results unequivocally demonstrate that, for the common PoTCs used in this work, the three processes proceed in the order: mRNA release, followed by tRNA release, followed by 70S splitting, the latter being the only process that absolutely requires GTP hydrolysis. In contrast, in the presence of an upstream SD sequence, which strengthens mRNA binding to the ribosome, both mRNA and tRNA release is slowed to the point that they proceed with the same rate as 70S splitting. Below we use these results, in combination with other related studies, to propose mechanisms for RRF/EF-G·GTP -induced breakdown of PoTCs in both the absence (common case) and presence (SD-case) of an upstream SD sequence.

Structural studies of RRF/EF-G·GTP-induced PoTC breakdown demonstrate that the ribosome is in a rotated state relative to a bare 70S ribosome and the deacylated tRNA is bound in a hybrid P/E position (29,39–41). A total of 14 bridges between 30S and 50S subunits have been identified within 70S ribosomes (39). The B2a and B3 bridges are disrupted in the presence of RRF and EF-G·GTP (39,40,42–44), disruptions that eventually lead to 70S splitting. Time-resolved studies have strongly suggested that 30S association with 50S proceeds via a multi-step process, with some bridges forming before others (45,46). Direct evidence that 70S splitting also proceeds via a multi-step process comes from cryoelectron microscopy studies of Fu *et al.* (40) who observed intermediate conformations during RRF/EF-G·GTP-dependent model PoTC breakdown, albeit one containing an upstream SD-sequence. Our results obtained with mRNAs lacking an SD sequence (common case) suggest that RRF/EF-G·GTP binding to the PoTC disrupts not only some ribosomal intersubunit bridges, but also the mRNA:tRNA codon:anticodon and tRNA:ribosome interactions. We speculate that, for the common case (Figure 3A), these initial disruptions are sufficient to induce mRNA release followed by tRNA release, but that disruption of additional intersubunit bridges are required for full splitting of the now vacant 70S ribosomes, which proceeds more slowly. A consequence of this speculation is that the bacterial cell would contain a significant steady-state population of vacant 70S ribosomes during active protein synthesis, some of which could participate directly in the initiation of protein synthesis on other mRNAs, in accord with results demonstrating that 70S splitting is not essential for such initiation (7-9). Indeed, recent results of ours demonstrate that RRF/EF-G·GTP binding stimulates mRNA and tRNA release from a model PoTC made using a ribosome with tethered subunits (7,47).

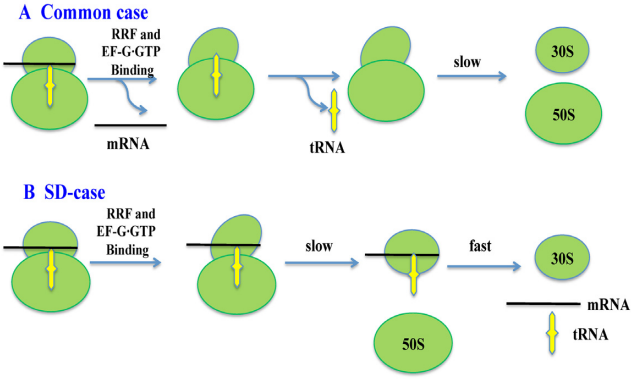

Figure 3. Proposed mechanisms of PoTC breakdown. (**A**) In the common case, partial disruptions of subunit:subunit contacts are sufficient to induce mRNA release followed by tRNA release, and 70S splitting. (**B**) In the SD-case, all three processes proceed at the same rate, with 70S splitting likely to be rate-determining.

mRNA binding to the ribosome is strengthened in the SD-case, and we propose (Figure 3B) that tRNA:mRNA interaction on the ribosome is maintained until full 70S splitting is accomplished, after which mRNA and tRNA are rapidly released into solution. This is consistent with the results of Karimi *et al.* (10) showing that tRNA dissociation from a model PoTC containing an upstream SD sequence requires GTP hydrolysis. In contrast, tRNA dissociation in the common case does not require GTP hydrolysis, since it precedes 70S splitting (Table 2). The dramatic differences in the mechanism of PoTC breakdown that we observe for ribosomes programmed with mRNA-F7 versus mRNA-SD-F7 (Table 2) raise interesting questions, to be addressed in future studies, as to how these differences would be affected by varying both the SD sequence and the spacing between the SD sequence and the stop codon.

Importantly, these proposed mechanisms for PoTC breakdown are consistent with ribosome profiling results determined in bacterial cells, which show that a strong SD-like sequence proximally upstream of the termination codon markedly increases ribosome occupancy at or just before the mRNA stop codon (16). Given the comparatively slow rate of ribosomal splitting [1.5–3 s^{-1} at 3 mM Mg^{2+}, Table 4; an *in vivo* rate of 5 s^{-1} has recently been estimated by Borg *et al.* (48)], as compared with the average rate of polypeptide elongation [~20 codons s^{-1} (49)], mRNA release that occurs simultaneously with 70S splitting, as in the SD-case, would be predicted to lead to high ribosome occupancy at the stop codon, as observed by Li *et al.* (16). By contrast, the much more rapid release of mRNA compared with ribosomal splitting in the common case would keep pace with elongation, and result in a lower occupancy at the stop codon of a typical mRNA lacking an upstream SD-like sequence. Indeed, such occupancies are observed to be only slightly elevated as compared with other open reading frame regions of mRNA (16,50–55).

Table 4. Rate constants for PoTC breakdown, 37°C

		Conditions			k_{app} (s^{-1})		
Source	#	SD	IF_3	Mg^{2+}	mRNA release	$tRNA^{Phe}$ release	Ribosome splitting
This work	1	–	–	3.0			2.8 ± 0.1
	2	–	–	5.0	25 ± 1	4.3 ± 0.2	0.47 ± 0.04
	3	+	–	5.0	0.51 ± 0.04	0.51 ± 0.04	0.50 ± 0.04
	4	–	+	5.0	25 ± 1	4.4 ± 0.3	0.36 ± 0.02
	5	–	–	7.5	4.3 ± 0.9	0.6 ± 0.1	0.09 ± 0.02
ref. (13)	6	+	+	7.0	0.03 ± 0.01	0.04 ± 0.01	0.3 ± 0.1[b]
	7	–	+	7.0			0.3 ± 0.1[b]
ref. (12)	8	+	+	3.0			1.51 ± 0.06
	9	+	–	3.0			1.60 ± 0.05
	10	(+)[a]	+	3.0			1.47 ± 0.06
ref. (11)	11	+	+	7.0		0.07	
ref. (48)	12	+	–	5.0			0.6[c]
							1.4

[a]Weak SD sequence.
[b]Determined using a FRET assay, the validity of which is questionable—see 'Discussion' section.
[c]Upper value: 1 μM RRF, 3 μM EF-G; lower value: 3 μM RRF, 3 μM EF-G.

Comparison with prior proposed kinetic mechanisms

The kinetic mechanism for the common case proposed in Figure 3A differs from those proposed by other groups who have studied this process in model PoTCs (4,11–13,33,34,56). Peske *et al.* (13) propose a model, with which Zavialov *et al.* (11) concur, in which 70S splitting is followed by simultaneous release of mRNA and tRNA from the 30S subunit, with the latter process being stimulated by IF3. On the other hand, Kaji *et al.* (4,37,41,47) posit that tRNA is released first, followed by 70S splitting and mRNA release, with some vagueness as to the order of the latter two reactions. Below we present an analysis of the reasons for these differences.

A summary of apparent rate constants determined for RRF/EF-G·GTP-dependent ribosome recycling is presented in Table 4. The only previous study reporting determinations for all three processes is that of Peske *et al.* (13) (Table 4, #6) but, importantly, it is for an mRNA containing a strong upstream SD sequence. These authors showed that the presence of an upstream SD sequence does not affect the rate constant they report for 70S splitting (Table 4, #7) and used this result to claim that 'the SD sequence has no influence on the mechanism of ribosome recycling.' Our results, demonstrating the very large effect the SD sequence has on the rates of both mRNA and tRNA release (Table 4, #2, #3), clearly demonstrate that this is not so. Nevertheless, Peske's results (Table 4, #6) should be comparable to ours (Table 4, #3) for PoTCs containing an upstream SD. Indeed, an important similarity for both sets of results is that the rates of mRNA and tRNA release are indistinguishable from one another. It is true that Peske's rates are much slower than ours, but this is mainly attributable to the higher [Mg^{2+}] in Peske's experiments, 7 mM in #6 versus 5 mM in #3 (Table 4). Indeed, based on the results in Table 4 showing that the presence of a strong SD sequence does not affect the rate of ribosome splitting (Table 4, #2 versus #3; #6 versus #7, #8 versus #10) but does result in all three processes proceeding at the same rate (Table 4, #3), we estimate that the rate constants for mRNA and tRNA dissociation for ribosomes programmed with mRNA-SD-F7 or mRNA-fl-SD-F7 at 7.5 mM Mg^{2+} will both be equal to 0.09 ± 0.02 s^{-1}, values that are similar in magnitude to those previously reported at 7.0 mM Mg^{2+} for mRNA release (Table 4, #6) and tRNA release (Table 4, #6, #11). The one significant difference in comparing Peske's results (Table 4, #6) to ours (Table 4, #3) is that Peske reports that 70S splitting occurs ∼10 times more rapidly than mRNA or tRNA release, whereas our results show all three rates to be the same. We attribute this apparent discrepancy to the fluorescence resonance energy transfer (FRET) assay Peske *et al.* employed to measure the rate of 70S splitting. In their work, 50S subunits and 30S subunits were labeled with a fluorescence donor and a fluorescence quencher, respectively, on surface lysines (3–5/per subunit) and the rate constant for increase in fluorescence intensity during PoTC breakdown, obtained by fitting the results to a *single* exponential, was interpreted as measuring the rate of 70S splitting. We consider this approach to be problematic, since FRET changes could arise from more rapid conformational changes in the 70S ribosome not resulting in splitting, especially given the large number of potential FRET interactions that could contribute to the overall FRET signal. In contrast, the light scattering approach that we employ provides a much more straightforward measure of 70S splitting, and yields rate constants that are reasonably consistent between our results (Table 4, #1) and those of Pavlov *et al.* (12) (Table 4, #8–#10) and Borg *et al.* (48) (Table 4, #12). We also note that Pavlov *et al.* (12) report that ribosomal splitting is ∼3- to 4-fold slower when cognate initiator $tRNA^{Met}$ replaces cognate $tRNA^{Phe}$ in the P-site of a PoTC, in both the common and SD-cases, which differs from our result showing the splitting rate to be unaffected by substituting cognate $tRNA^{Gly}$ for $tRNA^{Phe}$ (Table 2, common case). It is possible that this difference arises from the unique interactions of initiator $tRNA^{Met}$ with the P-site that are not found with elongator tRNAs (57–59).

While the model PoTCs employed by Peske *et al.* (13), Zavialov *et al.* (11), Pavlov *et al.* (12) and ourselves are similar to one another in having one ribosome bound per mRNA, Hirokawa *et al.* (37) employ a completely different model, prepared by puromycin-treatment of polysomes iso-

lated from cells. In addition, Hirokawa *et al.* infer a kinetic mechanism of PoTC recycling based on the different concentrations of an antibiotic needed for inhibition of specific steps in PoTC breakdown, measured at equilibrium (see above), rather than by direct rate measurements, as in the current work. Despite these differences, our current results agree with the conclusion of Hirokawa *et al.* that mRNA and tRNA are released from the PoTC prior to 70S splitting, while disagreeing with their conclusion that tRNA is released before mRNA. Here it may be relevant that the Hirokawa *et al.* model PoTC differs from ours in containing two bound tRNAs/ribosome rather than one (41), and in lacking a ribosome-bound stop codon. It is also possible that crosstalk among ribosomes bound to the same strand of mRNA within a polysome, possibly involving the formation or melting of mRNA secondary structures, could impede the rate of mRNA dissociation relative to dissociation from a single ribosome, or that different mRNA sequences could modulate the rates of mRNA and tRNA release to different extents.

Although our results are clear for the model PoTCs examined in this paper, we are mindful that they may not fully reflect the mechanism of PoTC breakdown *in vivo*. For example, as mentioned above, ribosome recycling from a polysome might proceed differently than from a monosome. It has also been suggested that incompletely folded full-length nascent protein newly released from a tRNA-bound ribosome might directly impact recycling (60). Clearly, further experiments will be required to resolve these points.

SUMMARY

We have shown, using direct, time-resolved, assays, that (i) for the common case model PoTCs employed in this work, the kinetic mechanism of PoTC breakdown proceeds in the order: mRNA release followed by tRNA release and then by 70S splitting; (ii) when there is a SD sequence upstream of the termination codon this mechanism is changed such that all three processes proceed with identical apparent rates, likely as a result of 70S splitting becoming rate determining; (iii) these two mechanisms are consistent with the effects of upstream SD-like sequences on ribosome profiling; (iv) differences between our proposed kinetic mechanism and those of earlier workers that were also based on rate measurements can be attributed both to an underestimation of the effects of an upstream SD sequence on PoTC breakdown as well as to the use of less straightforward measures of mRNA release and 70S splitting and (v) polysome structure and mRNA sequence could affect the relative order of mRNA and tRNA release. Our results support the view that, in general, the principal biological role of RRF and EF-G·GTP in catalyzing recycling is to effect the release of mRNA and tRNA from the PoTC, with the splitting of the 70S ribosome into 30S and 50S subunits being somewhat dispensable.

SUPPLEMENTARY DATA

Supplementary Data are available at NAR Online.

FUNDING

National Institutes of Health (NIH) [GM080376 to B.S.C.]; CBRI (to H.K.). Funding for open access charge: NIH.
Conflict of interest statement. None declared.

REFERENCES

1. Baba,T., Ara,T., Hasegawa,M., Takai,Y., Okumura,Y., Baba,M., Datsenko,K.A., Tomita,M., Wanner,B.L. and Mori,H. (2006) Construction of Escherichia coli K-12 in-frame, single-geneknockout mutants: the Keio collection. *Mol. Syst. Biol.*, **2**, doi:10.1038/msb4100050.
2. Yamamoto,N., Nakahigashi,K., Nakamichi,T., Yoshino,M., Takai,Y., Touda,Y., Furubayashi,A., Kinjyo,S., Dose,H., Hasegawa,M. *et al.* (2009) Update on the Keio collection of Escherichia coli single-gene deletion mutants. *Mol. Syst. Biol.*, **5**, 335.
3. Hirashima,A. and Kaji,A. (1972) Factor-dependent release of ribosomes from messenger RNA. Requirement for two heat-stable factors. *J. Mol. Biol.*, **65**, 43–58.
4. Hirokawa,G., Demeshkina,N., Iwakura,N., Kaji,H. and Kaji,A. (2006) The ribosome-recycling step: consensus or controversy? *Trends Biochem. Sci.*, **31**, 143–149.
5. Hirashima,A. and Kaji,A. (1972) Purification and properties of ribosome-releasing factor. *Biochemistry*, **11**, 4037–4044.
6. Hirashima,A. and Kaji,A. (1973) Role of elongation factor G and a protein factor on the release of ribosomes from messenger ribonucleic acid. *J. Biol. Chem.*, **248**, 7580–7587.
7. Orelle,C., Carlson,E.D., Szal,T., Florin,T., Jewett,M.C. and Mankin,A.S. (2015) Protein synthesis by ribosomes with tethered subunits. *Nature*, **524**, 119–124.
8. Yamamoto,H., Wittek,D., Gupta,R., Qin,B., Ueda,T., Krause,R., Yamamoto,K., Albrecht,R., Pech,M. and Nierhaus,K.H. (2016) 70S-scanning initiation is a novel and frequent initiation mode of ribosomal translation in bacteria. *Proc. Natl. Acad. Sci. U.S.A.*, **113**, E1180–E1189.
9. Qin,B., Yamamoto,H., Ueda,T., Varshney,U. and Nierhaus,K.H. (2016) The termination phase in protein synthesis is not obligatorily followed by the RRF/EF-G-dependent recycling phase. *J. Mol. Biol.*, **428**, 3577–3587.
10. Karimi,R., Pavlov,M.Y., Buckingham,R.H. and Ehrenberg,M. (1999) Novel roles for classical factors at the interface between translation termination and initiation. *Mol. Cell*, **3**, 601–609.
11. Zavialov,A.V., Hauryliuk,V.V. and Ehrenberg,M. (2005) Splitting of the posttermination ribosome into subunits by the concerted action of RRF and EF-G. *Mol. Cell*, **18**, 675–686.
12. Pavlov,M.Y., Antoun,A., Lovmar,M. and Ehrenberg,M. (2008) Complementary roles of initiation factor 1 and ribosome recycling factor in 70S ribosome splitting. *EMBO J.*, **27**, 1706–1717.
13. Peske,F., Rodnina,M.V. and Wintermeyer,W. (2005) Sequence of steps in ribosome recycling as defined by kinetic analysis. *Mol. Cell*, **18**, 403–412.
14. Savelsbergh,A., Rodnina,M.V. and Wintermeyer,W. (2009) Distinct functions of elongation factor G in ribosome recycling and translocation. *RNA*, **15**, 772–780.
15. Shine,J. and Dalgarno,L. (1974) The 3′-terminal sequence of *Escherichia coli* 16S Ribosomal RNA: complementarity to nonsense triplets and ribosome binding sites. *Proc. Natl. Acad. Sci. U.S.A.*, **71**, 1342–1346.
16. Li,G.W., Oh,E. and Weissman,J.S. (2012) The anti-Shine-Dalgarno sequence drives translational pausing and codon choice in bacteria. *Nature*, **484**, 538–541.
17. Kramer,P., Gabel,K., Pfeiffer,F. and Soppa,J. (2014) Haloferax volcanii, a prokaryotic species that does not use the Shine Dalgarno mechanism for translation initiation at 5′-UTRs. *PLoS One*, **9**, e94979.
18. Lakowicz,J. (1999) *Principles of Fluorescence Spectroscopy, Section 10.4*. Kluwer Academic/Plenum Publishers, NY.
19. Zhang,H., Ng,M.Y., Chen,Y. and Cooperman,B.S. (2016) Kinetics of initiating polypeptide elongation in an IRES-dependent system. *Life*, **5**, e13429.

20. Grigoriadou,C., Marzi,S., Kirillov,S., Gualerzi,C.O. and Cooperman,B.S. (2007) A quantitative kinetic scheme for 70 S translation initiation complex formation. *J. Mol. Biol.*, **373**, 562–572.
21. Wintermeyer,W. and Gualerzi,C. (1983) Effect of Escherichia coli initiation factors on the kinetics of N-AcPhe-tRNAPhe binding to 30S ribosomal subunits. A fluorescence stopped-flow study. *Biochemistry*, **22**, 690–694.
22. Kirillov,S.V., Makarov,E.M. and Semenkov,Y. (1983) Quantitative study of interaction of deacylated tRNA with Escherichia coli ribosomes. Role of 50 S subunits in formation of the E site. *FEBS Lett.*, **157**, 91–94.
23. Lill,R., Robertson,J.M. and Wintermeyer,W. (1986) Affinities of tRNA binding sites of ribosomes from Escherichia coli. *Biochemistry*, **25**, 3245–3255.
24. Lill,R. and Wintermeyer,W. (1987) Destabilization of codon-anticodon interaction in the ribosomal exit site. *J. Mol. Biol.*, **196**, 137–148.
25. Grajevskaja,R.A., Ivanov,Y.V. and Saminsky,E.M. (1982) 70-S ribosomes of Escherichia coli have an additional site for deacylated tRNA binding. *Eur. J. Biochem.*, **128**, 47–52.
26. Lancaster,L., Kiel,M.C., Kaji,A. and Noller,H.F. (2002) Orientation of ribosome recycling factor in the ribosome from directed hydroxyl radical probing. *Cell*, **111**, 129–140.
27. Wilson,D.N., Schluenzen,F., Harms,J.M., Yoshida,T., Ohkubo,T., Albrecht,R., Buerger,J., Kobayashi,Y. and Fucini,P. (2005) X-ray crystallography study on ribosome recycling: the mechanism of binding and action of RRF on the 50S ribosomal subunit. *EMBO J.*, **24**, 251–260.
28. Weixlbaumer,A., Petry,S., Dunham,C.M., Selmer,M., Kelley,A.C. and Ramakrishnan,V. (2007) Crystal structure of the ribosome recycling factor bound to the ribosome. *Nat. Struct. Mol. Biol.*, **14**, 733–737.
29. Yokoyama,T., Shaikh,T.R., Iwakura,N., Kaji,H., Kaji,A. and Agrawal,R.K. (2012) Structural insights into initial and intermediate steps of the ribosome-recycling process. *EMBO J.*, **31**, 1836–1846.
30. Liu,W., Shin,D., Tor,Y. and Cooperman,B.S. (2013) Monitoring Translation with Modified mRNAs Strategically Labeled with Isomorphic Fluorescent Guanosine Mimetics. *ACS Chem. Biol.*, **8**, 2017–2023.
31. Shin,D., Sinkeldam,R.W. and Tor,Y. (2011) Emissive RNA alphabet. *J. Am. Chem. Soc.*, **133**, 14912–14915.
32. Grunberg-Manago,M., Dessen,P., Pantaloni,D., Godefroy-Colburn,T., Wolfe,A.D. and Dondon,J. (1975) Light-scattering studies showing the effect of initiation factors on the reversible dissociation of Escherichia coli ribosomes. *J. Mol. Biol.*, **94**, 461–478.
33. Hirokawa,G., Nijman,R.M., Raj,V.S., Kaji,H., Igarashi,K. and Kaji,A. (2005) The role of ribosome recycling factor in dissociation of 70S ribosomes into subunits. *RNA*, **11**, 1317–1328.
34. Hirokawa,G., Iwakura,N., Kaji,A. and Kaji,H. (2008) The role of GTP in transient splitting of 70S ribosomes by RRF (ribosome recycling factor) and EF-G (elongation factor G). *Nuclelc Acids Res.*, **36**, 6676–6687.
35. Lin,J., Gagnon,M.G., Bulkley,D. and Steitz,T.A. (2015) Conformational changes of elongation factor G on the ribosome during tRNA translocation. *Cell*, **160**, 219–227.
36. Hansson,S., Singh,R., Gudkov,A.T., Liljas,A. and Logan,D.T. (2005) Crystal structure of a mutant elongation factor G trapped with a GTP analogue. *FEBS Lett.*, **579**, 4492–4497.
37. Hirokawa,G., Kiel,M.C., Muto,A., Selmer,M., Raj,V.S., Liljas,A., Igarashi,K., Kaji,H. and Kaji,A. (2002) Post-termination complex disassembly by ribosome recycling factor, a functional tRNA mimic. *EMBO J.*, **21**, 2272–2281.
38. Gorisch,H., Goss,D.J. and Parkhurst,L.J. (1976) Kinetics of ribosome dissociation and subunit association studied in a light-scattering stopped-flow apparatus. *Biochemistry*, **15**, 5743–5753.
39. Dunkle,J.A., Wang,L., Feldman,M.B., Pulk,A., Chen,V.B., Kapral,G.J., Noeske,J., Richardson,J.S., Blanchard,S.C. and Cate,J.H. (2011) Structures of the bacterial ribosome in classical and hybrid states of tRNA binding. *Science*, **332**, 981–984.
40. Fu,Z., Kaledhonkar,S., Borg,A., Sun,M., Chen,B., Grassucci,R.A., Ehrenberg,M. and Frank,J. (2016) Key intermediates in ribosome recycling visualized by time-resolved cryoelectron microscopy. *Structure*, **24**, 2092–2101.
41. Iwakura,N., Yokoyama,T., Quaglia,F., Mitsuoka,K., Mio,K., Shigematsu,H., Shirouzu,M., Kaji,A. and Kaji,H. (2017) Chemical and structural characterization of a model Post-Termination Complex (PoTC) for the ribosome recycling reaction: Evidence for the release of the mRNA by RRF and EF-G. *PLoS One*, **12**, e0177972.
42. Agrawal,R.K., Sharma,M.R., Kiel,M.C., Hirokawa,G., Booth,T.M., Spahn,C.M., Grassucci,R.A., Kaji,A. and Frank,J. (2004) Visualization of ribosome-recycling factor on the Escherichia coli 70S ribosome: functional implications. *Proc. Natl. Acad. Sci. U.S.A.*, **101**, 8900–8905.
43. Gao,N., Zavialov,A.V., Li,W., Sengupta,J., Valle,M., Gursky,R.P., Ehrenberg,M. and Frank,J. (2005) Mechanism for the disassembly of the posttermination complex inferred from cryo-EM studies. *Mol. Cell*, **18**, 663–674.
44. Zhang,Y., Mandava,C.S., Cao,W., Li,X., Zhang,D., Li,N., Zhang,Y., Zhang,X., Qin,Y., Mi,K., Lei,J., Sanyal,S. and Gao,N. (2015) HflX is a ribosome-splitting factor rescuing stalled ribosomes under stress conditions. *Nat. Struct. Mol. Biol.*, **22**, 906–913.
45. Hennelly,S.P., Antoun,A., Ehrenberg,M., Gualerzi,C.O., Knight,W., Lodmell,J.S. and Hill,W.E. (2005) A time-resolved investigation of ribosomal subunit association. *J. Mol. Biol.*, **346**, 1243–1258.
46. Shaikh,T.R., Yassin,A.S., Lu,Z., Barnard,D., Meng,X., Lu,T.M., Wagenknecht,T. and Agrawal,R.K. (2014) Initial bridges between two ribosomal subunits are formed within 9.4 milliseconds, as studied by time-resolved cryo-EM. *Proc. Natl. Acad. Sci. U.S.A.*, **111**, 9822–9827.
47. Quaglia,F., Kaji,H., Kaji,A. and Inokuchi,Y. (2017) *In vivo* and *in vitro* studies of RRF (ribosome recycling factor) revealed that its major function is to release mRNA from the post-termination complex and not splitting of the ribosomal subunits. *FASEB J.*, **31**(Suppl. 759.2), http://www.fasebj.org/content/31/1_Supplement/759.2.
48. Borg,A., Pavlov,M. and Ehrenberg,M. (2016) Complete kinetic mechanism for recycling of the bacterial ribosome. *RNA*, **22**, 10–21.
49. Kramer,G., Boehringer,D., Ban,N. and Bukau,B. (2009) The ribosome as a platform for co-translational processing, folding and targeting of newly synthesized proteins. *Nat. Struc. Mol. Biol.*, **16**, 589–597.
50. Ingolia,N.T., Ghaemmaghami,S., Newman,J.R. and Weissman,J.S. (2009) Genome-wide analysis in vivo of translation with nucleotide resolution using ribosome profiling. *Science*, **324**, 218–223.
51. Oh,E., Becker,A.H., Sandikci,A., Huber,D., Chaba,R., Gloge,F., Nichols,R.J., Typas,A., Gross,C.A., Kramer,G. *et al.* (2011) Selective ribosome profiling reveals the cotranslational chaperone action of trigger factor in vivo. *Cell*, **147**, 1295–1308.
52. Dunn,J.G., Foo,C.K., Belletier,N.G., Gavis,E.R. and Weissman,J.S. (2013) Ribosome profiling reveals pervasive and regulated stop codon readthrough in Drosophila melanogaster. *Elife*, **2**, e01179.
53. Guttman,M., Russell,P., Ingolia,N.T., Weissman,J.S. and Lander,E.S. (2013) Ribosome profiling provides evidence that large noncoding RNAs do not encode proteins. *Cell*, **154**, 240–251.
54. Davis,A.R., Gohara,D.W. and Yap,M.N. (2014) Sequence selectivity of macrolide-induced translational attenuation. *Proc. Natl. Acad. Sci. U.S.A.*, **111**, 15379–15384.
55. Juntawong,P., Girke,T., Bazin,J. and Bailey-Serres,J. (2014) Translational dynamics revealed by genome-wide profiling of ribosome footprints in Arabidopsis. *Proc. Natl. Acad. Sci. U.S.A.*, **111**, E203–E212.
56. Hirokawa,G., Kiel,M.C., Muto,A., Kawai,G., Igarashi,K., Kaji,H. and Kaji,A. (2002) Binding of ribosome recycling factor to ribosomes, comparison with tRNA. *J. Biol. Chem.*, **277**, 35847–35852.
57. Barraud,P., Schmitt,E., Mechulam,Y., Dardel,F. and Tisne,C. (2008) A unique conformation of the anticodon stem-loop is associated with the capacity of tRNAfMet to initiate protein synthesis. *Nucleic Acids Res.*, **36**, 4894–4901.
58. Shoji,S., Walker,S.E. and Fredrick,K. (2009) Ribosomal translocation: one step closer to the molecular mechanism. *ACS Chem. Biol.*, **4**, 93–107.
59. Kolitz,S.E. and Lorsch,J.R. (2010) Eukaryotic initiator tRNA: finely tuned and ready for action. *FEBS Lett.*, **584**, 396–404.
60. Das,D., Samanta,D., Bhattacharya,A., Basu,A., Das,A., Ghosh,J., Chakrabarti,A. and Das Gupta,C. (2017) A possible role of the full-length nascent protein in post-translational ribosome recycling. *PLoS One*, **12**, e0170333.